

Supplementary Materials for **Large-scale polymeric carbon nanotube membranes with sub-1.27-nm pores**

Robert L. McGinnis, Kevin Reimund, Jian Ren, Lingling Xia, Maqsd R. Chowdhury, Xuanhao Sun,
Maritza Abril, Joshua D. Moon, Melanie M. Merrick, Jaesung Park, Kevin A. Stevens,
Jeffrey R. McCutcheon, Benny D. Freeman

Published 9 March 2018, *Sci. Adv.* **4**, e1700938 (2018)

DOI: 10.1126/sciadv.1700938

This PDF file includes:

- Supplementary Text
- fig. S1. Experimental apparatus for RO testing.
- fig. S2. Experimental apparatus for gas permeation testing.
- fig. S3. Wireframe model of dye molecules.
- table S1. Manufacturer specifications for CNTs.
- table S2. Approximate enhancement factor for CNT composite membranes.
- References (33–40)

Supplementary Text

Characterization of the Polymeric Support

Membranes which were prepared without CNT (“process control”) were observed to exhibit less than ideal selectivity, but with gas permeance found to be uncorrelated with molecular mass and independent of pressure within the uncertainty of the measurements, indicating a dense polymer film with a thickness of approximately 75 nm.

The gas permeances of the CNT membranes were on the order of 5-10 times greater than the permeances of the process control membranes. Similarly, the pure water permeance of the process control membranes was on the order of 0.25 LMH/bar, with negligible salt rejection, versus a permeance of 5.1 LMH/bar for the CNT containing membranes. Published enhancement factors for water transport in CNTs are much higher than those for gas transport in CNTs (4, 33).

Estimation of Enhancement Factor

The enhancement factor (EF) is an empirical parameter which is defined simply as the ratio of observed flux, or permeability, to that predicted by Hagen-Poiseuille or Knudsen flow through an equivalently-dimensioned pore.

A review of SEM and TEM images indicate an approximate tube pore density of 250 ± 100 CNT/ μm^2 for the CNT membranes. The uncertainties are based primarily on uncertainty on the number of CNTs bundled in each apparent tube protrusion from the membrane surface and the overall tube coating density on the membrane at the macro scale. The Knudsen permeance through a pore of a given dimension is given by (34)

$$\frac{2}{3} \sqrt{\frac{8\pi}{MRT}} r^3 l^{-1} = P_{kd} \quad \text{Eq. S1}$$

where M is the molar mass, R is the gas constant, r is the radius of the pore, and l is its length. The permeance is expressed in units of $\text{mole} \cdot \text{pore}^{-1} \cdot \text{sec}^{-1} \cdot \text{Pa}^{-1}$.

The Hagen-Poiseuille permeance through a pore of a given dimension, in units of $\text{liter} \cdot \text{pore}^{-1} \cdot \text{sec}^{-1} \cdot \text{Pa}^{-1}$, is given by (35)

$$r^4 \frac{\pi}{8\mu} l^{-1} = P_{HP} \quad \text{Eq. S2}$$

where μ is the liquid viscosity.

The permeances predicted by the Hagen-Poiseuille (HP) and Knudsen (KD) equations are highly dependent on the radius of the pore, inversely dependent on the length of the pore, and linearly dependent on the number of pores per unit area. The wall thickness of a CNT is approximated by the Van der Waals radius of a carbon atom (1.7 Å) (6), which is subtracted from the stated outer radius. We assume that the manufacturer stated values for arc discharge CNTs, summarized in

table S1, and independently measured diameters (20) continue to be accurate after treatment of CNT. Ignoring any potential correlation between average length and diameter, the enhancement factors for the CNT membranes may be approximated and are shown in table S2.

Evaluation of Transport Regimes for Gas Flow

Transport through the process-control polymer matrix, as previously described, is between the Knudsen selectivity and the solution-diffusion selectivity for polysulfone, and the transport through the CNT membranes is less selective than Knudsen flow.

Some pressure dependency in the permeance of gases through the CNT membranes was observed. Typically, pressure-dependent permeance is indicative of viscous flow, which is given in mole·pore⁻¹·sec⁻¹·Pa⁻¹, by (35)

$$\frac{\epsilon}{l\tau} \frac{r^2}{8\mu RT} = \frac{J_{viscous}}{p_m} = P_{viscous} \quad \text{Eq. S3}$$

where ϵ and τ are the porosity and tortuosity of the membrane pores, and p_m is the mean pressure in the pores. Viscous flow is inversely proportional to the viscosity of the transporting gas in Equation S3, so the ratio of the flux of two pure gases (i.e., the pure gas selectivity) should be proportional to the inverse ratio of their viscosities. No such relation was found for transport through the CNT composite membrane (Fig. 3B), indicating that viscous flow is not a significant transport mechanism for gases in the CNT-composite membranes.

In a previous study of gas transport through small CNT inner diameters embedded in a zeolite membrane structure, pressure dependent permeance relationships were also observed, which the authors suggested was most likely due to the increased contribution of surface diffusion of gases, relative to Knudsen flow, for tube diameters below 1 nm (27). Surface diffusion, unlike Knudsen flow, can show pressure dependence due to the influence of pressure on adsorption on the tube wall, which is an important component of this mode of transport. It is likely that the same effects are responsible for the pressure dependency observed in this study.

Ionic Strength Effects in Salt and Dye Rejection

Previously, Fornasiero et al. identified that ionic solutes are well-retained by ~1.6 nm inner diameter (ID) CNTs at low ionic strength (<10 mM for KCl), but that rejection precipitously drops at higher ionic strength (25, 36). Similarly, Akbari et al. demonstrated that graphene oxide membranes with a layer spacing of ~9.5 Å have high retention of dilute solutions of anionic dyes, but slightly less rejection of cationic dyes at the same concentration (37). To reduce the effects of charge screening and Donnan exclusion on the rejection of probe dyes, the rejection of the dyes was analyzed in the presence of 2000 ppm NaCl (34 mM). If a difference in rejection is observed between the two conditions, then Donnan exclusion is playing a role in overall analyte rejection. If no difference is observed, as in the case of chlorophyllin copper sodium salt, it is expected that steric exclusion is the dominant mechanism.

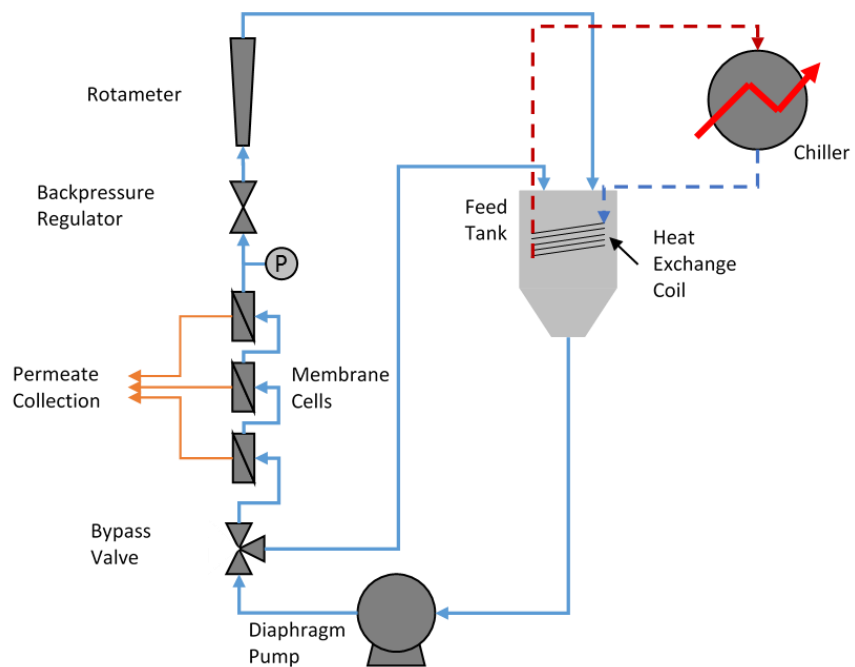


fig. S1. Experimental apparatus for RO testing.

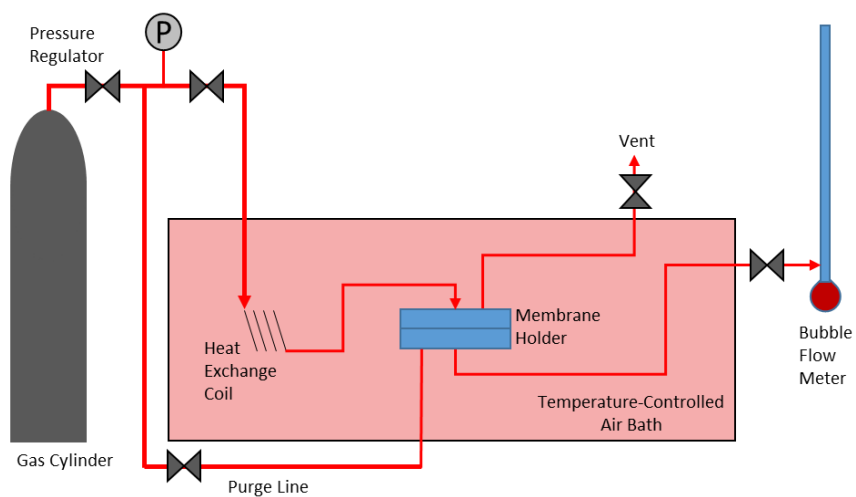


fig. S2. Experimental apparatus for gas permeation testing.

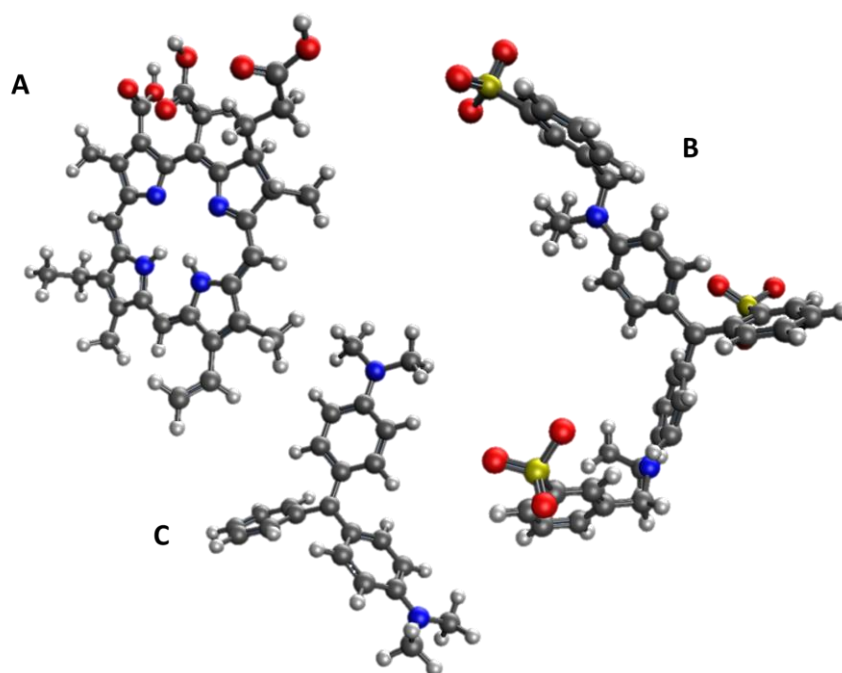


fig. S3. Wireframe model of dye molecules. Molecular models have been modified to remove counter-ions. Chlorophyllin anion (Cu not present) (38) (A); FD&C Blue #1 anion (39) (B); Malachite green cation (40) (C).

table S1. Manufacturer specifications for CNTs.

Carbonaceous Purity	>90%
Length	500-1500 nm
Outer Diameter	1.55 (mean)
Bundle Diameter	4-5 nm

table S2. Approximate enhancement factor for CNT composite membranes.

Water EF (relative to HP flow)	He EF (relative to KD flow)	N ₂ EF (relative to KD flow)
1000	70	30